Thermal resistance and temperature characteristics of GaAs/$Al_{0.33}Ga_{0.67}As$ quantum-cascade lasers

Vincenzo Spagnolo, Mariano Troccoli, and Gaetano Scamarcio[a)]
INFM, Dipartimento Interateneo di Fisica, Università e Politecnico di Bari, Via Amendola 173, 70126 Bari, Italy

Cyrille Becker, Geneviève Glastre, and Carlo Sirtori
Thomson-CSF, Laboratoire Central de Recherches, 91404 Orsay, France

(Received 30 October 2000; accepted for publication 3 January 2001)

We report on the determination of thermal resistance, facet temperature profile, and heat flux of GaAs/$Al_{0.33}Ga_{0.67}As$ quantum-cascade lasers operating in pulsed mode, using a microprobe band-to-band photoluminescence technique. The thermal resistance of epilayer-side mounted lasers is ~30% smaller than that of substrate-side mounted ones. The dependence of the thermal resistance on the injection conditions and its correlation with the output power is also reported. © *2001 American Institute of Physics.* [DOI: 10.1063/1.1351850]

Quantum-cascade (QC) lasers based on GaAs/AlGaAs have undergone a rapid development over the last few years.[1–3] In the wavelength range 9–12 μm at 77 K, output powers as high as ~1.5 W have been reported.[2] Still, the highest operating temperatures reported are 260 K in pulsed operation[2] and 30 K in continuous wave.[4] The main limiting factors are the large electrical power typically required for operation, and the low thermal conductivity characteristic of ternary alloys and multiple heterostructures.[5,6] These effects lead to an active region temperature well above the heat sink.[7,8]

In this letter we report the determination of the thermal resistance and lattice temperature of GaAs/$Al_{0.33}Ga_{0.67}As$ QC lasers during pulsed operation. We used microprobe band-to-band photoluminescence[8,9] to compare epilayer-side and substrate-side mounted devices with identical epilayer structure. The absence of surface recombination processes in unipolar devices such as QC lasers allow the use of the facet temperature as a close estimate of the device internal one.[10,11]

A GaAs/$Al_{0.33}Ga_{0.67}As$ laser structure (wafer V1966) was grown by molecular beam epitaxy on GaAs substrate doped to $2-3\times10^{18}\,cm^{-3}$. The active layer consists of a 1.5 μm thick stack of 36 three-wells active regions designed for emission at $\lambda=9.4\,\mu$m and is sandwiched between two 3.5 μm thick GaAs layers n doped to $8\times10^{16}\,cm^{-3}$ and two 1 μm thick GaAs plasmon cladding layers heavily n-doped to $5\times10^{18}\,cm^{-3}$. The devices were mounted on the cold finger of a helium flow microcryostat whose temperature was controlled with a Si diode mounted close to the laser. The microprobe photoluminescence (PL) apparatus is identical to that used in Ref. 8. The main characteristics are: the ~1 μm laser spot diameter, the liquid N_2 cooled Si CCD detection system and the piezo x-y translation stage with 0.1 μm precision. The 476.2 nm line of a Kr^+ laser was focused on the samples with an incident power density below $10^4\,W/cm^2$.

Figure 1 shows representative photoluminescence spectra of different regions of the laser front facets. The spectrum of the low doped GaAs layer [see Fig. 1(a)] shows the characteristic band of bulk GaAs peaked at 1.504 eV, with a bandwidth of 14 meV. Luminescence from the active region [see Fig. 1(b)] is dominated by a band peaked at 1.603 eV, with a bandwidth of 16 meV, associated with ground state band-to-band transitions. The ~0.1 eV blueshift with respect to Fig. 1(a) is due to quantum confinement effects in the GaAs/AlGaAs multiple heterostructure. Figure 1(c) shows the PL spectrum of the plasmon guide layer. The peak position (1.57 eV) and the bandwidth (~70 meV) correspond to heavily n-doped GaAs.

The local lattice temperature is determined following the method outlined in Ref. 8, where the shift of the PL peak energy E_p is compared with a calibration curve [see Fig. 1(d)]. The rather strong temperature dependence ($dE_p/dT=0.3-0.4\,meV/K$) at $T>70\,K$, gives an uncertainty value of ±0.4 K, significantly smaller than ±10 K achievable with microprobe Raman technique.[12]

Figure 2 shows the schematics of laser facets for

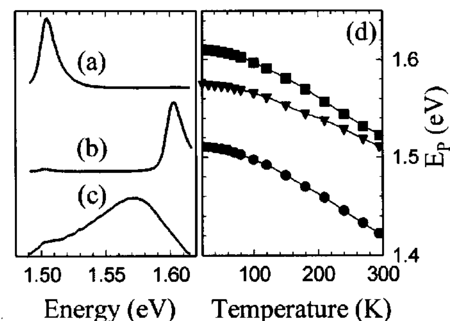

FIG. 1. Characteristic microprobe photoluminescence spectra taken from the cladding layer (a), the active region (b), and the plasmon guide layer (c) of a QC laser front facet. (d) Temperature dependence of the plasmon guide region (▼), active region (■), and cladding layer (●) photoluminescence peak position, obtained varying the heat sink temperature T_H at zero current. The determination of the peak energy E_p was carried out by fitting the PL spectra in a region 25 meV around E_p with a second-order polynomial. The continuous lines in (d) are obtained with the empirical relation $E_p(T)=E_p(0)-\alpha T^2/(\beta+T)$, which accurately reproduces the band gap shrinkage with temperature.

[a)]Author to whom correspondence should be addressed; electronic mail: scamarcio@fisica.uniba.it

0003-6951/2001/78(9)/1177/3/$18.00 © 2001 American Institute of Physics

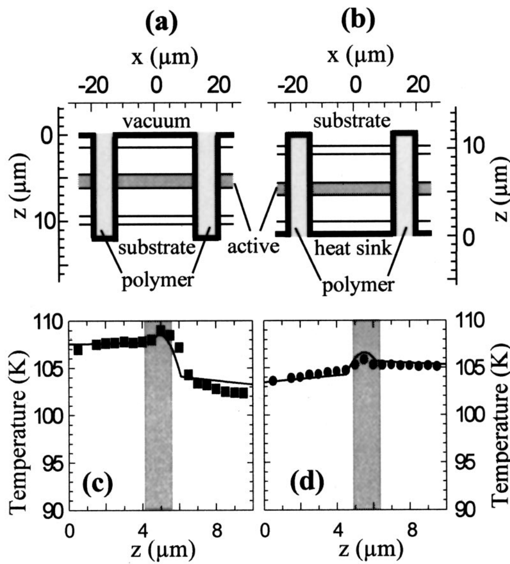

FIG. 2. Schematics of QC laser facets for a substrate-side (a) and an epilayer-side (b) mounted devices. Measured facet temperature profiles (symbols) of substrate-side (c) and epilayer-side (d) mounted QC lasers, at heat sink temperatures of 90 K. The solid lines are best fit calculations using a two-dimensional heat flow model employing the values 1.65, 0.1, 0.87, 3.2, 0.4, and 6.5 $W K^{-1} cm^{-1}$ for the heat conductivity of bulk GaAs, oxide layer, contact layer, In solder, polymer, and Cu, respectively. An electrical power of 1.38 W was dissipated into the devices, corresponding to an injected current of 2 A, with a pulse width of 100 ns and a repetition rate of 1 MHz.

substrate-side (a) and epilayer-side (b) mounted devices. Ridge waveguides 1 mm long and 25 μm wide are defined using photolithographic techniques and reactive ion etching. Lateral trenches are filled with polymer to planarize the device. The laser structures were indium soldered onto metal holders extending the solder bonding to the very end of the laser ridge. This avoids facet overheating and the formation of ''hot spots.''[7] The local temperature measured at different positions along the facet center axis parallel to the growth direction for the substrate-side (c) and the epilayer-side (d) mounted device is shown in Figs. 2(c) and 2(d). The two devices show markedly different thermal behaviors. The active region in the epilayer-side mounted laser is cooler than in the substrate-side mounted one, with a difference of 3.5 K between the two peak temperatures. The temperature difference at the boundaries of the active region, $\Delta T_{AR}=T(z=4.5\,\mu m)-T(z=6\,\mu m)$, is significantly larger for the substrate-side mounted device ($\Delta T_{AR}=4$ K) than for the epilayer-side mounted one ($\Delta T_w=-0.5$ K). These values are related with the disparity in the heat flux along the z axis and indicate an improved heat extraction towards the cladding layer close to the heat sink ($z<4.5\,\mu$m) in the epilayer-side mounted device.

The heat fluxes can be obtained by fitting a two-dimensional model of heat diffusion to the experimental results of Figs. 2(c) and 2(d), leaving the heat conductivity in the active region, k_{AR}, as the only fitting parameter and employing appropriate values for the heat conductivity of the different materials composing the device (see caption of Fig. 2). We set the heat sink temperature as boundary condition and found best agreement with the value $k_{AR}=(5.5\pm0.5)10^{-2}$ W/(K cm). As expected, due to the presence of interfaces and phonon interference effects, the heat conductivity of the active region is considerably smaller than that of the constituent materials.[5,6] The results of the fitting procedure show that, in the epilayer-side mounted device, ~56% of the total heat flows towards the cladding layer closest to the heat sink ($z<4.5\,\mu$m). The residual heat reaches the heat sink through the GaAs substrate and the lateral channels ($|x|>20\,\mu$m), whereas the heat flux through the trenches filled with polymer is negligible. In the substrate-side mounted device most of the heat is dissipated through the GaAs substrate and only ~27% of the total heat flows towards the top of the ridge ($z<4.5\,\mu$m) before reaching the heat sink through the contact layers and the lateral channels.

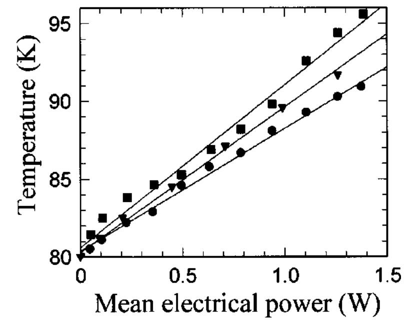

FIG. 3. Active region mean temperature as a function of the electrical mean power measured at $f=1$ MHz; (■) substrate-side mounted QC laser, pulse width $\Delta t=100$ ns; (●) epilayer-side mounted device, $\Delta t=100$ ns; (▼) epilayer-side device, $\Delta t=200$ ns. The lines are linear fits to the data. Their slopes are the thermal resistances.

The dissimilarity in the heat flow configurations arises from the difference between the thermal resistances of the two devices. This quantity has been obtained from the data of Fig. 3, showing the mean temperature of the active region as a function of the mean injected power. We observe a linear increase of the temperature in the range 80–95 K, while keeping fixed the heat sink temperature at $T_H=80$ K, and the repetition rate at $f=1$ MHz. The two different slopes measured with a pulse width of $\Delta t=100$ ns correspond to thermal resistance values $R=11.2\pm0.5$ K/W for the substrate side and $R=7.8\pm0.5$ K/W for the epilayer-side mounted lasers. In the latter device we found that at $\Delta t=200$ ns, $f=1$ MHz the thermal resistance increases to $R=9.5\pm0.5$ K/W. In order to study the dependence on the pulse width at constant duty cycle, we probed the epilayer-side mounted device with $\Delta t=200$ ns and $f=500$ kHz, and we found $R=8.6\pm0.5$ K/W. This 10% increase of the thermal resistance with respect to the case $\Delta t=100$ ns, $f=1$ MHz, can be explained considering the larger temperatures reached during longer pulses, which in turn cause a decrease of the thermal conductivity.[5,6]

Figure 4(a) shows the influence of the pulse repetition rate f on the active region mean temperature measured by micro-PL for an epilayer-side mounted QC laser. Deviation from linearity in Fig. 4(a) becomes evident for $f>300$ kHz and corresponds to an increase of R with the repetition rate. These findings are consistent with the notion that the excess thermal energy is transferred from the semiconductor chip to the heat sink in several μs. Our results are in qualitative agreement with time-resolved heat transport measurements in GaAs/AlGaAs diode lasers.[13] The low heat dissipation rate of heterostructure devices with respect to bulk materials

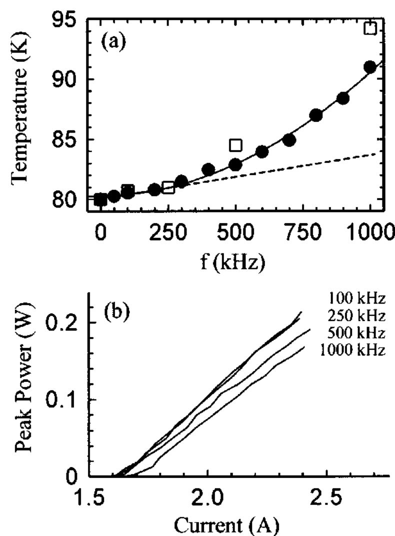

FIG. 4. (a) Active region mean temperature for an epilayer-side mounted QC laser as a function of the repetition rate; (●) temperatures measured by micro-PL with an injected current of 2 A and a pulse width of 100 ns, (□) temperatures extrapolated from the analysis of the threshold current temperature dependence. The solid and dotted curves are guides for the eye. (b) Peak power output vs current characteristics measured at 80 K with a pulse width of 100 ns and repetition rates as specified in the figure. The laser output from the front facet is collected with a $f/0.8$ optical system. The estimated collection efficiency is $\eta = 0.5$.

is related with the reduction of the phonon group velocity perpendicular to the layers.[14]

The frequency dependence of the thermal resistance leads to a performance deterioration in terms of output power at increasing frequencies. Figure 4(b) shows the optical power-current characteristics measured as a function of f. We observe a decrease in the slope efficiency and an increase of the threshold current with the repetition rate. This behavior correlates well with the data of Fig. 4(a). In fact, from the characteristic temperature $T_0 = 100\,\mathrm{K}$, extracted from the temperature dependence of the threshold current density at low duty cycles, and the measured threshold currents of Fig. 4(b), we estimated the active region temperatures at threshold (~1.6 A). The open squares in Fig. 4(a) show the extrapolated temperatures at $I = 2$ A, using the thermal resistance value extracted from Fig. 3.

In conclusion, the PL microprobe study of the facet temperature profile of GaAs/AlGaAs-based QC lasers shows the lower thermal resistance and the superior thermal dissipation capability of epilayer-side mounted devices. The presented analysis will allow to design QC laser structures with improved heat dissipation capability.

This work is partly supported by INFM—Project No. PRA98 ''SUPERLAS'' and MURST Cluster 26 ''Materiali Innovativi'' Project No. P5BW2. The work performed at Thomson-CSF was partly funded by the European Community under the BRITE/EURAM ''UNISEL'' Project (Contract No. CT-97-0557).

[1] C. Sirtori, P. Kruck, S. Barbieri, P. Collot, J. Nagle, M. Beck, J. Faist, and U. Oesterle, Appl. Phys. Lett. **73**, 3486 (1998).
[2] C. Sirtori, H. Page, C. Becker, P. Kruck, G. Glastre, and M. Stellmacher, *Proceedings of the Conference on Lasers and Electro-Optics, OSA Technical Digest* (Optical Society of America, Washington, DC, 2000), p. 265.
[3] P. Kruck, H. Page, C. Sirtori, S. Barbieri, M. Stellmacher, and J. Nagle, Appl. Phys. Lett. **76**, 3340 (2000).
[4] W. Schrenk, N. Finger, S. Gianordoli, E. Gornik, and A. Strasser, Appl. Phys. Lett. **77**, 3328 (2000).
[5] G. Chen, Phys. Rev. B **57**, 14958 (1998).
[6] W. S. Capinski, H. G. Maris, T. Ruf, M. Cardona, K. Ploog, and D. S. Katzer, Phys. Rev. B **59**, 8105 (1999).
[7] C. Gmachl, A. M. Sergent, A. Tredicucci, F. Capasso, A. L. Hutchinson, D. L. Sivco, J. N. Baillargeon, S. N. G. Chu, and A. Y. Cho, IEEE Photonics Technol. Lett. **11**, 1369 (1999).
[8] V. Spagnolo, M. Troccoli, G. Scamarcio, C. Gmachl, F. Capasso, A. Tredicucci, A. M. Sergent, A. L. Hutchinson, D. L. Sivco, and A. Y. Cho, Appl. Phys. Lett. (in press).
[9] D. C. Hall, L. Goldberg, and D. Mehuys, Appl. Phys. Lett. **61**, 384 (1992).
[10] R. Schaltz and C. G. Bethea, J. Appl. Phys. **76**, 2509 (1994).
[11] R. Puchert, A. Bärwolff, U. Menzel, A. Lau, M. Voss, and T. Elsasser, J. Appl. Phys. **80**, 5559 (1996).
[12] W. C. Tang, H. J. Rosen, P. Vettiger, and D. J. Webb, Appl. Phys. Lett. **58**, 557 (1991).
[13] M. Voos, C. Lier, U. Menzel, A. Bärwolff, and T. Elsaesser, J. Appl. Phys. **79**, 1170 (1996).
[14] S. Tamura, Y. Tanaka, and H. J. Maris, Phys. Rev. B **60**, 2627 (1999).